water

MDPI

Article

Iron Isotopic Composition of Suspended Particulate Matter in Hongfeng Lake

Xiaodi Zheng [1,2], Yanguo Teng [1,2] and Liuting Song [1,2,*]

[1] College of Water Sciences, Beijing Normal University, Beijing 100875, China; zhengxiao91@163.com (X.Z.); teng1974@163.com (Y.T.)

[2] Engineering Research Center of Groundwater Pollution Control and Remediation Ministry of Education of China, Beijing 100875, China

* Correspondence: ltsong@bnu.edu.cn; Tel.: +86-010-5880-2736

Received: 19 December 2018; Accepted: 2 February 2019; Published: 24 February 2019

Abstract: The geochemical study of iron isotopes is of great significance to comprehensively understand the surface material circulation process and its environmental effects in surface and subsurface environments. Eutrophic lakes are an important part of the surface and subsurface environment; however, knowledge of the geochemical behaviour and fractionation mechanism of iron isotopes in the biogeochemical cycling of eutrophic lakes is still scarce. In this study, a eutrophic lake with seasonal anaerobic characteristics (Hongfeng Lake) was selected as the study object to systematically analyse the iron isotope composition of suspended particles in lake water and the main tributaries in different seasons. The results show that the value of δ^{56}Fe in Hongfeng Lake is between −0.85‰ and +0.14‰, and the value of δ^{56}Fe has a high linear correlation with Fe/Al, indicating that the continental source material carried by the main inflow tributaries of the lake has an important influence on the source of iron in the lake. And Hongfeng Lake is moderately eutrophic lakes. Algal bloom and the content of chlorophyll a (Chl-a) are high, combined with the high correlation between Chl-a and the value of δ^{56}Fe, which indicates that the growth of algae has an important influence on the change in the iron isotope composition of suspended particulate matter (SPM) in lake water and that the adsorption and growth absorption of Fe by algae are the main reason for the change in the value of δ^{56}Fe; therefore, Fe isotope can be used to trace the lake's biological action. For the lake and its inflow tributaries, δ^{56}Fe values are higher in summer than in winter. The variation in the δ^{56}Fe value of SPM with lake depth is more distinct in summer than in winter. In addition, there is a distinct thermocline in summer, which leads to hydrochemical stratification. Moreover, according to a linear correlation analysis, the content of dissolved organic matter (DOC) in Hongfeng Lake's upper and lower water bodies, respectively, has a high correlation with the value of δ^{56}Fe. Specifically, the correlation is positive in the upper water but negative in the lower water, which indicates that the difference in algae metabolism patterns between the upper and lower water bodies of Hongfeng Lake plays an important role in the iron isotope composition of SPM. The composition of the iron isotope in SPM is altered by organic adsorption and growth absorption of algae in the upper water. With an increase in depth, degradation becomes the main process. In addition, the value of δ^{56}Fe is low and that of Fe/Al is high in the water bottom, which indicates that a "ferrous-wheel" cycle forms at the bottom of the water.

Keywords: iron isotope; SPM; eutrophic lake; algae

1. Introduction

Iron is the fourth most abundant element in the Earth's crust and exists widely in the atmosphere, soil, rivers and oceans, plants, and animals. Additionally, iron is one of the main micronutrients

of plants and animals and plays an important role in the growth and reproduction of plants and algae [1,2]. Iron is one of the main factors that affects the primary productivity of lakes. In particular, bioavailable iron is an important factor in the control of the species and growth rate of algae [3,4]. Iron sources are highly abundant in lake ecosystems, for example, river input, atmospheric deposition, sediment resuspension and reduction and remigration of sediments [5,6]. Moreover, the distribution of iron in lakes is complicated by the hydrodynamic characteristics of the lake itself as well as the various input terminals and various circulation processes that occur within the lake [7,8]. In recent years, with the development of multiple collector inductively coupled plasma mass spectrometry (MC-ICP-MS) analysis technology, great progress has been made in iron isotope technology and its application to aquatic ecosystems, but it is still necessary to use Fe isotopes to comprehensively understand the biogeochemical cycling of Fe [9–15].

To date, iron isotopes have been studied in lake ecosystems, but δ^{56}Fe has rarely been used to trace the biogeochemical cycle of eutrophic lakes. Teutsch et al. [16] studied the strong isotopic variation of Fe (II) in volcanic Lake Nyos using iron isotope techniques. At present, research on the changes in iron isotope composition in suspended particulates has mostly focused on river systems. Such studies on the Amazon River and its tributaries show that, compared to terrestrial materials, which contain large amounts of low-suspended organic matter, rivers are enriched with light Fe isotopes. In rivers containing large amounts of suspended particulate matter (SPM), the δ^{56}Fe value is close to the terrestrial value, as reported by Poitrasson et al. [17], which is consistent with previous studies on the Amazon and Nile rivers [18,19]. Although many studies have shown that SPM is enriched with light Fe isotopes compared to terrestrial sources, some studies show that the size distribution and activity of colloidal particles in the dissolved phase as well as the varying activity of the redox zone among different study areas will lead to abnormal results [20–23]. Among the researchers associated with those studies, Ingri et al. [20] noted that the δ^{56}Fe value of organic colloids in the dissolved phase was −0.13‰, while the δ^{56}Fe value of hydroxide colloids was as high as +0.3‰. Meanwhile, Chen et al. [24] found that anthropogenic influences caused the SPM in the Seine River in France to be enriched with light Fe isotopes. The correlation between δ^{56}Fe and DOC/Fe in SPM shows that the soluble Fe from natural sources is mainly combined with organic colloids. The low DOC/Fe and δ^{56}Fe values in the iron mixture may be affected by anthropogenic Fe hydroxide or sulfide colloids [24]. Therefore, anthropogenic pollution will also affect the δ^{56}Fe value of rivers. Song et al. [25] found that the δ^{56}Fe value of SPM in rivers and lakes in southern China varied from −1.36‰ to +0.07‰, with ferrous-wheel redox reaction and coal mine wastewater discharge as the main reasons for the negative δ^{56}Fe value. Therefore, biological and abiotic processes such as redox reactions, mineral dissolution, organic matter mixing, adsorption/desorption and biological uptake are the main processes that lead to the change in iron isotope composition between dissolved and particulate phases [26,27]. In these processes, dissolved Fe (II) will partially oxidize and precipitate to particulate Fe (III), such as a hydroxide or sulfide, and partial Fe (II) will remain in the solution, resulting in a maximum difference of 3.9‰ in the iron isotope value [28].

SPM in lakes is a mixture of inorganic, organic and biological detritus, phytoplankton, bacteria, etc., that are trapped at 0.22 μm or 0.45 μm by membranes. Therefore, Hongfeng Lake is selected as the research object of this study, which is a karst plateau eutrophic lake and a seasonally anoxic artificial lake. Hypoxia in the bottom water appears in summer, while the water is mixed in winter [29,30]. Through the determination of iron isotopes in suspended particles and algae in lakes and the inflowing rivers, the differences in iron isotopes in different end members of the lake system were observed, and the controlling factors for the differences in the compositions of these isotopes were studied. Additionally, a theoretical basis is provided for the application of iron isotopes in the study of lake biogeochemical processes.

2. Study Site, Sampling, and Analytical Details

2.1. Study Site

Hongfeng Lake is a seasonally anoxic artificial lake located in the suburbs approximately 31.5 km southwest of Guiyang, China. The lake has a surface area of 57.2 km^2, a maximum depth of 45 m, a total volume of 9.18×10^8 m^3, and a residence time of 0.325 year. The water collection zones of Hongfeng Lake's exposure strata are Permian and Triassic. The carbonatite of the Triassic is the most widely distributed, followed by clastic rock. The major soil types of the area are lime yellow soil and a proportion of rice soil with the characteristic of vertical zoning. The land use of the Hongfeng Lake basin is dominated by woodland and farmland, which account for more than 60% of the total area. The plants of the area include coniferous plantation, evergreen broad-leaved forest, shrub and agricultural tillage field. The average annual precipitation is 1183.22 mm, and the average annual temperature is 14.1 °C.

The recharge water sources of Hongfeng Lake are river and meteoric water. Hongfeng Lake is divided into the upstream south lake and the downstream north lake. Yangchang River (YCR), Maxian River (MXR) and Houliu River (HLR) are the main tributaries for the south lake, and the only effluent river of Hongfeng Lake is Maotiao River (MTR). Fertilizer plant wastewater flows through the river.

2.2. Sampling

The sample area is shown in Figure 1. This included the lake area of Hongfeng Lake and the tributaries around the lake. Samples were collected from Houwu (HW) station located upstream south of Hongfeng Lake. The samples were collected in the summer of 2006 and the winter of 2007.

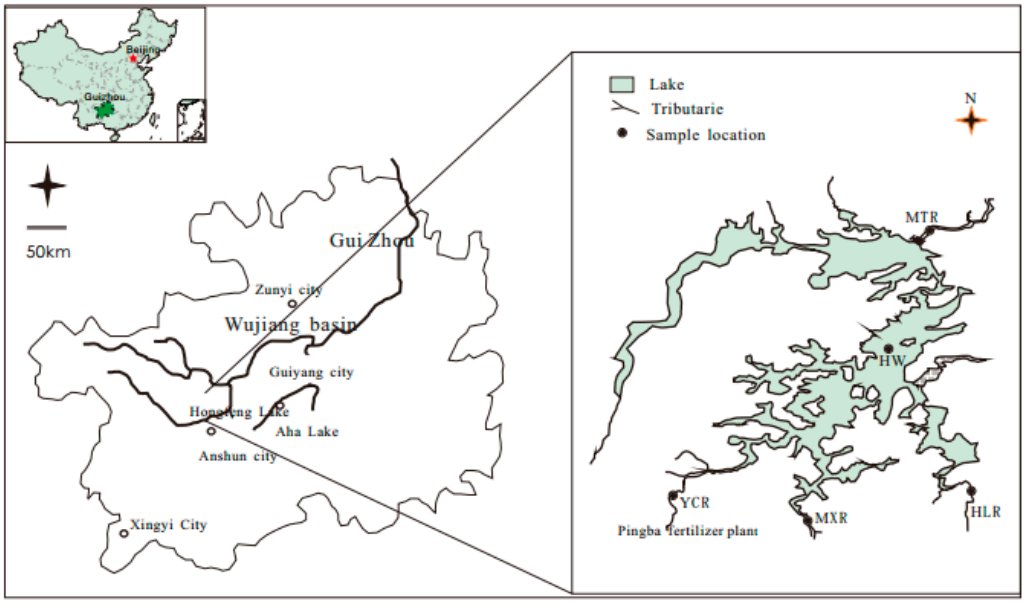

Figure 1. Location and sampling map of Hongfeng Lake, southwestern China.

All the wares used in the laboratory and in field were carefully cleaned. Polyethylene bottles, tubes and HDPE bottles for sample collections were all soaked with 6 N HCl (hydrochloric acid) for more than three days and then rinsed with deionized water and 18.2 MΩ Milli-Q water. The filters (Millipore HA, 0.45 µm, 47 mm, MilliporeSigma, Burlington, MA, USA) were treated three times with 1 M double-distilled HCl, alternating with 18.2 MΩ Milli-Q water. The brown glass bottles were firstly acid cleaned and then combusted, together with the glass microfiber filters (Whatman, GF/F, 25 mm, Maidstone, UK) used for dissolved organic carbon (DOC) samples, in the muffle furnace at 450 °C for 4 h. A multi-parameter sensor was used to determine the pH, water temperature (T) and electrical

conductivity (EC); red-bromocresol green was used as a mixed indicator; and filtered samples were acidified with 0.02 N HCl. Samples for measurement of cations and anion filters in the field and filtered samples were analyzed for cation and metal concentrations were acidified to pH < 2. The anions were measured by ion chromatography (Dionex, ICS-90, Sunnyvale, CA, USA), and sulfate and nitrate concentrations had detection limits of 2.08 μM and 3.22 μM, respectively. Cations were measured by Vista MPX ICP-OES. Trace elements were measured by GV Platform ICP-MS.

Samples for the measurements of iron isotopic compositions were filled in the sampling bucket of high density polyethylene and returned to the laboratory. Samples were filtered through 0.45 μm Millipore HA membrane filters. The filters with SPM were stored in polyethylene tubes in the refrigerator. Atmospheric particles were collected with a homemade polyethylene rainwater sampler without pollution, and the rainwater was then filtered as soon as possible. Additionally, any particulate matter obtained was regarded as atmospheric particles, and membrane filters were stored in a refrigerator. Samples for phytoplankton were automatically collected and selected while wearing polyethylene gloves. The samples were then cleaned with lake water and pure water without chemical reagents.

2.3. Iron Isotope Analysis

Samples were prepared in a clean room of the State Key Laboratory of Environmental Geochemistry of the Institute of Chemistry of Chinese Academy of Sciences. All work was completed in a room with class 1000 and class 100 laminar flow hoods. Milli-Q water (18.2 MΩ) was used throughout the procedures. High-purity acid was obtained by double distillation of hydrochloric acid and hydrofluoric acid, and the hydrogen peroxide product was electronically pure [31,32].

2.3.1. Sample Dissolution

Lake SPM, river SPM and atmospheric particles were digested for iron isotope testing. And all samples were first dried at 50 °C in an oven, the interior of which was covered with Teflon materials. Then, these samples were soaked in 3 mL aqua regia and 0.5 mL concentrated HF (hydrofluoric acid) for 48 h in acid-cleaned Teflon beakers (7 ml, Savillex, Eden Prairie, MN, USA). The beakers were left on a hot plate and dried at 80 °C. Another 3 mL of aqua regia and 0.5 mL of concentrated HF were added, and the closed beaker was left on a hot plate for 72 h at 140 °C. The samples with a high content of silicate had 1 mL HF added to them. The plant samples were cleaned with deionized water and Millipore ultrapure water, placed in a polyethylene bag and stored in a refrigerator for 24 h. These samples were then freeze-dried, ground to powder, and digested using the same method used for SPM. The digested samples were left on a hot plate to dry, and the procedure was sequentially repeated three times with concentrated HCl to eliminate HNO_3 and HF. Finally, each sample was redissolved into 7 N HCl + 0.001% H_2O_2 for chemical purification.

2.3.2. Chemical Purification

Anion-exchange chromatography was performed with a polypropylene column filled with AG MP-1 resin (Bio-Rad, 100–200 mesh). Chemical purification was carried out using procedures similar to those of Maréchal et al. [33] and Song et al. [25]. The matrix was striped with 35 mL of 7 N HCl + 0.001% H_2O_2, and Fe was eluted with 20 mL of 2 N HCl + 0.001% H_2O_2. The exchange chromatograph could be regenerated for further use. The iron eluent was placed in 25 mL Teflon beakers and left on a hot plate to dry at 100 °C. The final Fe eluate was dissolved in 1% HNO_3 at a concentration of 5 ppm for isotope analysis. And samples which had a high substrate content were then purified a second time by anion-exchange chromatography to obtain.

2.3.3. Mass Spectrometry

Iron isotope analyses were performed on a Nu Plasma instrument HR MC-ICP-MS, and the carrier gas was argon. The RF (radio frequency) power was 1300 W delivered via a desolvating nebulizer DSN-100 system, with concentrations ranging from 5 to 10 ppm in 1% HNO_3. The $\delta^{56}Fe$ signal intensity was 18 V. The standards and samples were cleaned with 10% HNO_3 for 3 min and 1% HNO_3 for 2 min. Data were collected automatically by Unix-based operating system control software provided by Dr. Belshaw from the University of Oxford. Each group of data was collected as 2 data points, and the integral time of each point was 20 s. A background determination of 20 s was conducted before data collection for each group. The standard-sample bracketing (SSB) method was used in sample testing to correct the fractionation of the instrument. The standard-sample concentrations matched within 5%. The performance of the instrument was assessed by repetitive measurements of an internal lab standard (CAGS-Fe3) relative to the Fe isotope reference material IRMM-014. The long-term reproducibility of iron isotopic measurements by MC-ICP-MS defined from the 16 months' replicate analyses were 0.11% for $\delta^{57}Fe$ and 0.08% for $\delta^{56}Fe$. The detailed operating conditions and the performance of isotope measurements were described by Zhu et al. [34,35]. Fe isotope data are reported in $\delta^{x}Fe$ as parts per thousand deviations relative to IRMM-014:

$$\delta^{x}Fe = [(^{x}Fe/^{54}Fe)_{sample}/(^{x}Fe/^{54}Fe)_{IRMM} - 1] \times 1000. \quad (1)$$

2.4. Chlorophyll-a as an Index for the Divided Lake Nutrition Level

The modified Carlson index (TSI_M) was put forward as a trophic status index after extensive research (Table 1). The index is calculated as follows [36]:

$$TSI_M(Chl) = 10\left(2.46 + \frac{lnChla}{ln2.5}\right). \quad (2)$$

Table 1. Eutrophication Assessment Criteria of TSI_M [37].

Carlson Index	Lake Nutrition Level
0~20	Oligotrophic
20~50	Mesotrophic
50~70	Eutrophic
70~100	Heavy Eutrophic

3. Results

3.1. Basic Water Chemical Parameters in the Lake and Its Tributaries in Hongfeng Lake

The test results pertaining to water temperature, pH value, and dissolved oxygen content in Hongfeng Lake in summer and winter are listed in Table 2 and Figure 2. In winter, the lake water was in a mixed state, and the water chemical index showed no distinct profile of change characteristics (Figure 2). Unlike that in winter, the temperature of the lake surface in summer was much higher than that of the lake bottom. The difference was approximately 10 °C, and obvious thermal stratification was observed (Table 2). Both pH and DO showed a downward trend with an increase in the lake water depth. Starting at 12 m, the pH and DO concentration in the bottom water decreased significantly, with average values of 7.5 and 1.3 $mg{\cdot}L^{-1}$ (Figure 2 and Table 2), respectively, which indicated an anaerobic state. The thermal stratification of lakes in summer lead to chemical stratification, and indicators such as conductivity (EC), dissolved silicon (H_4SiO_4) and DOC showed distinct profiles of change characteristics. Among them, EC and H_4SiO_4 levels at the surface of the lake were relatively low—293.2 $mg{\cdot}L^{-1}$ and 1.07 $mg{\cdot}L^{-1}$, respectively. As the depth of the lake increased, these values showed significant upward trends, especially in the bottom water near the water–sediment interface

(Figure 2). In contrast to EC and H_4SiO_4, the DOC content in the surface lake was higher (4.9 mg·L^{-1}) and gradually decreased with increasing lake water depth. Toward the oxygen-deficient area at the bottom, the upward trend again appeared (Figure 2 and Table 2). The results of a chlorophyll content test in Hongfeng Lake showed that the average content of Chl-a in winter was 8.9 μg·L^{-1}, and the content of Chl-a in summer was higher. The surface water was approximately 42.1 μg·L^{-1}, which gradually decreased with an increase in depth. Finally, Chl-a dropped below 10 μg·L^{-1} (average value 6.4 μg·L^{-1}) in the bottom anaerobic zone exceeding a depth of 12 m (Figure 2 and Table 2). Based on the average concentration of Chl-a in the layer for lake water production (<10 m), the TSI_M of Hongfeng Lake was obtained by the modified Carson index method. The TSI_M value of winter was 50.1, while that in summer was 60.2, indicating a moderately eutrophic state (Table 1). The determination of Cl^-, SO_4^{2-}, and NO_3^- content in Hongfeng Lake and its tributaries showed that the concentration of SO_4^{2-} in the tributary was between 0.49 and 0.92 mM, while the concentration of SO_4^{2-} in the lake was between 0.58 and 1.01 mM (Table 2). The Cl^- concentration of the tributary was between 0.03 and 0.63 mM, and the Cl^- concentration of the lake varied from 0.14 to 0.20 mM (Table 2). The NO_3^- concentration of the tributary was between 0.01 and 0.32 mM, and the NO_3^- concentration of the lake varied from 0 to 0.11 mM (Table 2). The concentrations of Cl^- and NO_3^- in MXR and HLR were similar to or lower than those in the lake, while the concentrations of Cl^- and NO_3^- in YCR were higher than those in the lake in winter or summer. This trend may be related to YCR's sewage inflow from fertilizer plants.

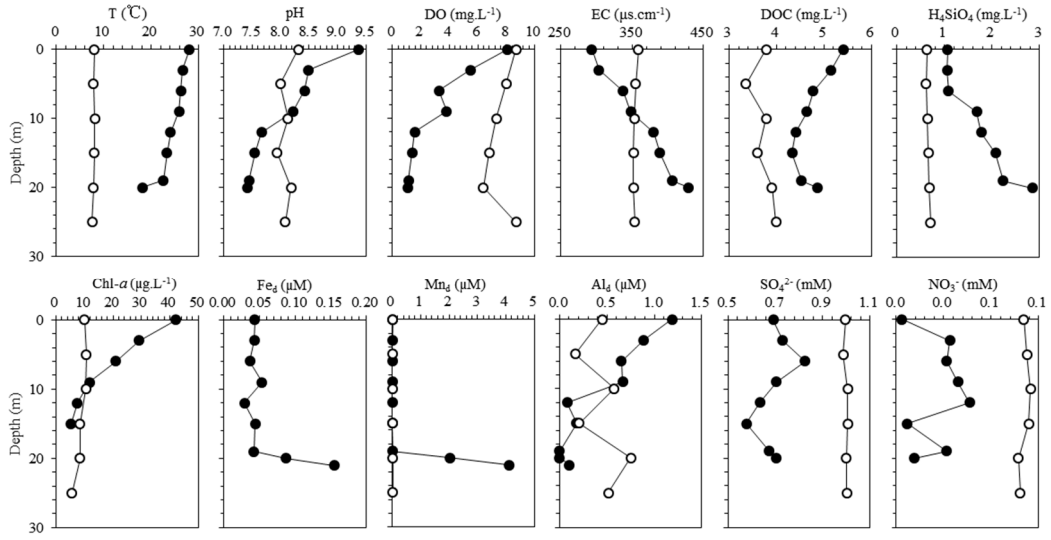

Figure 2. Depth profiles of environmental parameters and chemical data in the summer and winter in Hongfeng Lake.

Table 2. Environmental parameters and chemical data for Hongfeng Lake and its tributaries.

Sample Station	Date	Depth (m)	T (°C)	pH	DO ($mg \cdot L^{-1}$)	EC ($\mu s \cdot cm^{-1}$)	DOC ($mg \cdot L^{-1}$)	H_4SiO_4 ($mg \cdot L^{-1}$)	Chl-a ($\mu g \cdot L^{-1}$)	Fe_d (μM)	Mn_d (μM)	Al_d (μM)	SO_4^{2-} (μM)	NO_3^- (μM)	Cl^- (μM)
HW	Aug. 2006	0	28.10	9.37	8.10	293.20	4.91	1.07	42.10	0.04	0.01	1.19	0.69	0.00	0.17
HW	Aug. 2006	3	26.60	8.49	5.48	303.20	4.65	1.06	29.23	0.04	0.01	0.89	0.73	0.05	0.17
HW	Aug. 2006	6	26.30	8.42	3.27	337.40	4.27	1.09	21.06	0.04	0.00	0.65	0.83	0.04	0.18
HW	Aug. 2006	9	25.90	8.21	3.80	348.00	4.14	1.68	11.74	0.05	0.01	0.67	0.70	0.05	0.17
HW	Aug. 2006	12	24.10	7.66	1.58	380.40	3.90	1.78	7.50	0.03	0.01	0.08	0.63	0.06	0.15
HW	Aug. 2006	15	23.30	7.54	1.39	389.10	3.83	2.08	5.23	0.04	0.01	0.18	0.58	0.01	0.14
HW	Aug. 2006	19	22.60	7.44	1.12	406.50	4.02	2.23		0.04	0.01	0.00	0.67	0.04	0.16
HW	Aug. 2006	20	18.10	7.42	1.09	429.30	4.36	2.85		0.09	2.02	0.00	0.70	0.01	0.18
HW	Aug. 2006	21								0.16	4.10	0.10			
HW	Jan. 2007	0	8.00	8.31	8.70	359.00	3.28	0.63	9.91		0.02	0.45	1.00	0.11	0.19
HW	Jan. 2007	5	7.80	7.99	8.00	354.70	2.86	0.61	10.61		0.01	0.16	0.99	0.11	0.19
HW	Jan. 2007	10	8.10	8.13	7.30	352.90	3.28	0.64	10.52		0.01	0.57	1.00	0.11	0.19
HW	Jan. 2007	15	8.00	7.94	6.80	351.70	3.10	0.67	8.36		0.01	0.20	1.01	0.11	0.19
HW	Jan. 2007	20	7.80	8.18	6.40	352.00	3.40	0.68	8.34		0.02	0.75	1.00	0.10	0.19
HW	Jan. 2007	25	7.50	8.08	8.70	353.80	3.49	0.71	5.58		0.03	0.52	1.00	0.10	0.20
YCR	Aug. 2006	0	26.50	7.37	7.8	447.60	3.29	5.13		0.68	0.32	2.18	0.61	0.09	0.33
YCR	Jan. 2007	0	3.40	7.08	7.70	481.60	2.17	10.34			0.36	5.33	0.83	0.32	0.63
MXR	Aug. 2006	0	26.30	8.04	9.6	300.60	7.16	1.37		0.23	0.38	0.16	0.56	0.01	0.03
MXR	Jan. 2007	0	4.20	7.67	8.50	360.50	2.45	1.53			0.04	0.18	0.85	0.04	0.11
HLR	Aug. 2006	0	24.90	8.07	9.7	393.90	5.08	2.87		0.44	0.10	<0.01	0.49	0.01	0.09
HLR	Jan. 2007	0	3.90	9.72	8.40	402.50	3.04	1.28			0.23	0.37	0.92	0.07	0.16
MTR	Aug. 2006	0	20.70	7.49	3.1	464.40	5.27	2.41		0.08	0.11	<0.01	1.21	0.00	0.25
MTR	Jan. 2007	0	6.90	7.42	10.00	384.90	2.95	0.69			0.05	0.15	1.18	0.20	0.20

3.2. Dissolved Fe, Mn, and Al Contents in Hongfeng Lake and Its Tributaries

Similarly to the basic water chemistry index, due to the mixed effect of lake water, the dissolved Mn and Al in Hongfeng Lake in winter showed no obvious profile changes (Table 2 and Figure 2). In the summer, the concentrations of dissolved Fe and Mn in the upper lake were low, 0.04 μM and 0.01 μM, respectively. And the profile change was not distinct. However, the concentrations of dissolved Fe and Mn near the water–sediment interface showed a significant increasing trend. In particular, the dissolved Mn increased from 0.01 μM to 4.10 μM. In contrast, the concentration of dissolved Al in the lake surface was as high as 1.19 μM and gradually decreased with an increase in depth. The average content in the bottom water was only 0.03 μM. For the tributary rivers, the contents of dissolved Fe, Mn, and Al in summer varied from 0.23 μM to 0.68 μM, from 0.10 μM to 0.38 μM, and from 0 μM to 2.18 μM, respectively. In winter, the concentrations of dissolved Mn and Al ranged from 0.04 μM to 0.36 μM and from 0.18 μM to 5.33 μM, respectively, which were higher than in the summer.

3.3. Fe, Mn, and Al Contents and δ^{56}Fe Values of SPM in Hongfeng Lake and Its Tributaries

The test results pertaining to the Fe, Mn, and Al content and δ^{56}Fe values of SPM collected from the lake and rivers are listed in Table 3. Because the dissolved Fe concentration was low, the δ^{56}Fe value was not determined.

Table 3. Iron isotopic composition and chemical composition of trace ions Fe, Mn and Al of Hongfeng Lake and its inflowing rivers.

Sample	Date	Depth	δ^{56}Fe	δ^{57}Fe	Fe	Mn	Al	Fe/Al	Mn/Al
Station		(m)	(‰)	(‰)	(μmol·L^{-1})	(μmol·L^{-1})	(μmol·L^{-1})		
HW	Aug. 2006	0	0.13	0.23	0.86	0.09	2.31	0.37	0.04
HW	Aug. 2006	3	0.10	0.13	2.07	0.10	4.44	0.47	0.02
HW	Aug. 2006	6	0.06	0.08	0.96	0.11	2.42	0.40	0.04
HW	Aug. 2006	9	0.03	0.11	1.56	0.71	3.30	0.47	0.21
HW	Aug. 2006	12	0.04	0.11	1.57	0.61	3.37	0.47	0.18
HW	Aug. 2006	15	0.14	0.24	0.61	0.38	1.78	0.34	0.22
HW	Aug. 2006	19	0.07	0.15	1.23	1.26	2.55	0.48	0.49
HW	Aug. 2006	20	−0.18	−0.19	2.19	0.23	2.11	1.04	0.11
HW	Aug. 2006	21	−0.14	−0.21					
HW	Jan. 2007	0	−0.04	0.00	0.97	0.13	1.97	0.49	0.07
HW	Jan. 2007	5	−0.04	0.00	1.03	0.18	2.02	0.51	0.09
HW	Jan. 2007	10	−0.08	−0.14	1.02	0.19	1.96	0.52	0.09
HW	Jan. 2007	15	0.09	0.16	0.53	0.09	1.56	0.34	0.06
HW	Jan. 2007	20	−0.85	−1.24	1.44	0.17	2.99	0.48	0.06
HW	Jan. 2007	25	−0.03	−0.05	1.49	0.17	4.14	0.36	0.04
YCR	Aug. 2006	0	−0.18	−0.25	2.00	0.34	5.67	0.35	0.06
YCR	Jan. 2007	0	−0.49	−0.71	2.47	0.09	3.88	0.64	0.02
MXR	Aug. 2006	0	0.10	0.21	2.33	0.51	4.67	0.50	0.11
MXR	Jan. 2007	0	0.03	0.03	0.85	0.02	1.09	0.79	0.02
HLR	Aug. 2006	0	0.06	0.12	2.27	0.16	7.62	0.30	0.02
HLR	Jan. 2007	0	0.04	0.06	1.71	0.11	5.69	0.30	0.02
MTR	Aug. 2006	0	−0.46	−0.68	0.23	1.66	0.24	0.98	6.90
MTR	Jan. 2007	0	−0.06	−0.11	0.54	0.22	1.56	0.35	0.14
Phytoplankton	Jan. 2007	0	0.36	0.53				0.52	0.05
Aerosol-1	Oct. 2006		0.08	0.14				0.37	0.01
Aerosol-2	Oct. 2006		0.12	0.17				0.39	0.03

3.3.1. Riverine SPM

Differences in the contents of Fe, Mn, and Al for different SPM samples in different seasons were observed (Table 3). The Fe contents of SPM in YCR, MXR, and HLR, which flow into the lake in the summer, were 2.00 μM, 2.33 μM and 2.27 μM, respectively. The Mn contents of SPM was low, 0.34 μM, 0.51 μM, and 0.16 μM, respectively. During the dry season in winter, the Fe and Mn contents of SPM were generally reduced. In particular, the decrease in the Mn content was the most significant, which was between 30% and 96% (Table 3). The M/Al ratio can be used as an indicator of detrital or non-detrital inputs of M through a comparison with the detrital background ratios [10]. The unpolluted soil in Guiyang was shown to have a Fe/Al ratio of 0.28. The average Fe/Al ratio and Mn/Al ratio

of atmospheric sediment particles were 0.38 and 0.02, respectively. The Fe/Al ratios of SPM in YCR, MXR, and HLR in summer were 0.35, 0.50, and 0.30, respectively. Additionally, the ratios of SPM in winter were 0.64, 0.79, and 0.30, respectively. Therefore, the Fe/Al ratios of YCR and MXR were slightly higher than the background value of the basin. The Mn/Al ratio of SPM in the tributaries in summer was 0.02~0.11 and that in winter was 0.02. In summer, the Mn/Al ratios in YCR and HLR were slightly higher than the local background values. The δ^{56}Fe value of SPM in the tributaries varied from −0.46‰ to +0.06‰ in summer, while it varied from −0.49‰ to +0.04‰ in winter. The δ^{56}Fe value of SPM (−0.18‰) in YCR in summer was significantly higher than that (−0.49‰) in winter, while the δ^{56}Fe value of SPM in MXR and HLR (0.03‰~0.10‰) did not change appreciably in summer or winter and was close to the average value (0.09‰) of the continental crust.

3.3.2. Lake SPM

The average Fe and Mn contents of SPM in Hongfeng Lake (HW station) in summer were 1.38 μM and 0.44 μM, respectively. Additionally, the average contents of Fe and Mn in winter were 0.93 μM and 0.16 μM, respectively. Therefore, the summer content was higher than the winter content overall (Table 2). The profile distribution showed that the Fe and Mn contents exhibited a zigzag distribution in summer, and the winter changes were relatively insignificant (Figure 3). As shown in Figure 3, the δ^{56}Fe value of SPM in summer varied from −0.18‰ to +0.14‰, and the δ^{56}Fe value of SPM in winter varied from −0.85‰ to +0.09‰. The winter values were lower than the summer values. In particular, the bottom layer appeared to have an extremely negative value of −0.85‰. However, the δ^{56}Fe value of SPM in the upper layer did not change appreciably in winter, showing a downward trend with a range of −0.04‰~−0.08‰ from the surface layer to approximately 10 m. Then, an extremely negative value appeared at a depth of 20 m after a higher value was observed at 15 m. The δ^{56}Fe value of SPM increased significantly to −0.03‰ near the water–sediment interface. In the summer, the δ^{56}Fe value of SPM tended to decrease gradually from the surface to approximately 10 m. A higher value +0.14‰ appeared at approximately 15 m and then gradually decreased as the depth increased. The most negative value, −0.18‰, occurred at 20 m (Table 2 and Figure 3). The δ^{56}Fe values of atmospheric particles were measured to be 0.08‰ and 0.12‰, and algae was measured to be +0.36‰.

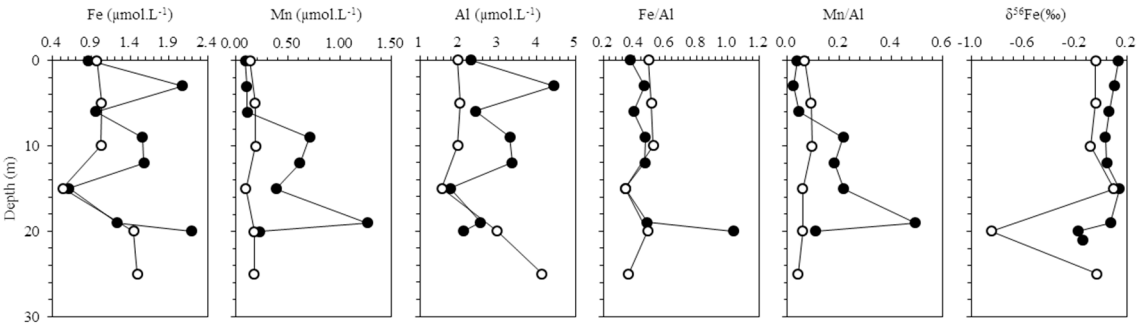

Figure 3. Depth profiles of Fe, Mn, and Al; Fe/Al and Mn/Al ratios; and δ^{56}Fe values of suspended particulate matter in summer and winter in Hongfeng Lake.

4. Discussion

4.1. Hydrochemical Stratification of Hongfeng Lake

The thermal stratification of lake water plays an important role in the vertical exchange of nutrients between dissolved and particulate substances in the system, the bioavailability of microbial substrates, and the vertical distribution, migration, and transportation of phytoplankton, fish, and other higher nutrient levels [38–41]. During the stratification of Hongfeng Lake in summer, the hydrochemical characteristics of the water show that the river input controlled the hydrochemical composition of the surface layer of the lake, resulting in characteristics such as a high pH, high DO, and high DOC, which is

similar to the results found in a study of Aha Lake in the same region by Song et al. [25]. DOC is the main energy source of microbial metabolism in water, which can be decomposed into smaller molecules and become nutrients for algae [42]. The concentration of dissolved organic matter is controlled by natural and anthropogenic inputs as well as by autochthonous processes [43,44]. The contents of DOC in YCR, MXR and HLR was 3.29 mg·L^{-1}, 7.16 mg·L^{-1} and 5.08 mg·L^{-1}, respectively. The input contribution of DOC was 4.33 mg·L^{-1} based on the calculation of the inflow volume of each tributary into the lake, and the DOC content of the surface lake in summer was 4.91 mg·L^{-1}, demonstrating that autochthonous processes of the lake also have important effects on the DOC content of the surface water. Studies have shown that during algal growth, the exudation of DOC by algae enters the water, especially when nutrients are scarce [45,46]. According to the TSI_M value of the lake, Hongfeng Lake is a moderately eutrophic lake. The surface water has a Chl-a value of up to 42.10 μg·L^{-1} in summer, and the Chl-a contents in upper lake and the corresponding δ^{56}Fe values show a good positive correlation (R^2 = 0.98) (Figure 4). However, the NO_3^- and DSi contents in the lake are relatively low, which indicates that the autochthonous DOM of algal origin produced during the mass propagation of algae in summer may be an important source of DOC in surface lake water. When entering the anoxic zone at the bottom of the lake (>15 m), the DOC appears to gradually increase again. Furthermore, EC and DSi also increase gradually, while the pH value, NO_3^- and SO_4^{2-} of lake water are low, which indicates that the bottom layer of the lake is dominated by organic matter degradation. In the water near the water-sediment interface in particular, the dissolved Fe and Mn are greatly increased. This finding indicates that the diffusion of sediment pore water to the overlying water may also have an important influence on the water chemistry characteristics of the bottom water [25,47].

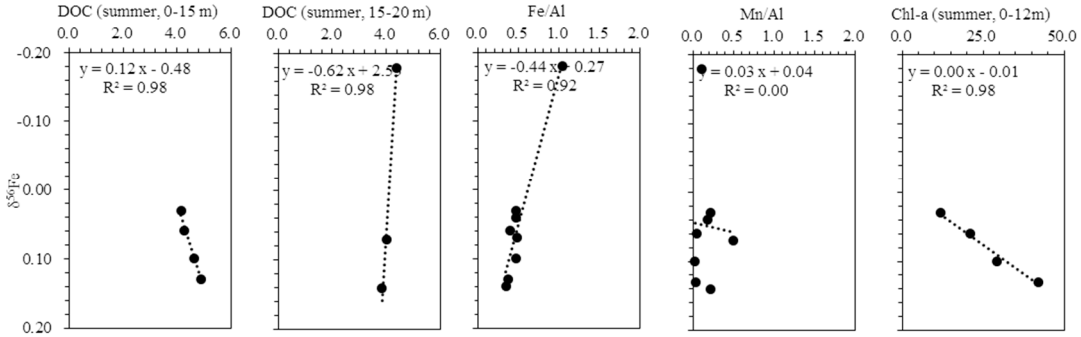

Figure 4. Correlations between δ^{56}Fe values and the corresponding Chl-a, DOC, Fe/Al, and Mn/Al values in the summer SPM in Hongfeng Lake.

4.2. Source Control of Iron Isotopes in Hongfeng Lake

The material source in the lake system is affected by regional geochemical properties, lake geochemical processes, biological effects, etc., which include atmospheric deposition, terrestrial input, sediment resuspension, and biological effects [7,48,49]. Moreover, particulate iron exists in the aquatic environment through processes such as biological uptake, degradation, adsorption and desorption, and precipitation-dissolution in biological and abiotic forms [50–52]. Hongfeng Lake has a surface area of 57.2 km^2 and a water depth of more than 20 m, which implies that wind-induced resuspension of sediment will have limited contributions. In addition, river input is an important source of lake SPM. During the settlement of particles in the lake or estuary, fractionation of the Fe isotopic composition of SPM may occur due to size separation and sorption/desorption processes. However, we roughly estimated the river flow [53,54] and the iron isotope value of the river SPM and concluded that the input contribution value of the river is approximately −0.03‰. The average iron isotope in the upper lake water is 0.08‰, which is relatively high. Combined with the fact that the lake particulate matter Fe/Al ratio range (0.34–1.04) and the river particulate matter Fe/Al ratio range (0.30–0.98) are similar, and through correlation analysis, it is found that the iron isotope composition in the suspension of

Hongfeng Lake in summer has a strong correlation with Fe/Al (R^2 = 0.81), indicating that the river is a negative input of iron isotope source to the lake (Figures 5 and 6).

Iron exists in the lake environment in the form of Fe (II) and Fe (III). The formation of Fe (III) compounds by oxidation, sulfuration and organic mineralization of Fe (II) is the main cause of the formation of particulate iron from biological processes in lakes [55]. Moreover, Klar's research indicates that most biological activities will make the particles rich in heavy iron isotopes ($\Delta^{56}Fe_{pFe\text{-}dFe} < -0.54‰$), and the occurrence of anomalies may be related to the type of phytoplankton [28]. In addition, in the enrichment of heavy Fe isotopes, the bond energy of the iron-complexed coordination bond (C–O–Fe) has a stronger effect on the organic complex of Fe (III) than on the iron hydroxide bond (Fe–O–Fe). The $\Delta^{56/54}Fe_{Fe(III)\text{-}organic\text{-}Fe(III)\text{-}H2O}$ value in the organic coordination bond mixing process is within 1‰, and the Fe (III) organic matter of the small molecule is more concentrated than in the Fe (III) organic substance. The lakes examined in this study are moderately eutrophic lakes with strong algae growth and high chlorophyll content, especially at the surface (42.10 $\mu g \cdot L^{-1}$). Chlorophyll a content can be used to evaluate lake biological activity levels, and existing studies have shown a certain correlation between biological activity process and $\delta^{56}Fe$ value [28]. Furthermore, Radic's research has shown that the isotope fractionation range of iron particles formed through the bio-absorption process is $\Delta^{56}Fe_{phyto\text{-}DFe} = -0.25 \pm 0.10‰$ to $-0.13 \pm 0.11‰$ (2SD) when the chlorophyll a content of the marine environment is the highest. In this study, the $\delta^{56}Fe$ value of algae in Hongfeng Lake was 0.36‰, and there was a high correlation between the $\delta^{56}Fe$ value and Chl-a in upper lake (R^2 = 0.98). Combined with the influence of the river input on the iron isotopic composition of lakes, the changes in DOC, EC and DSi in summer indicate that the growth of autochthonous algae may also be an important source of SPM in lakes (Figures 5 and 6). The study conducted by Liang Lili et al. on Zn isotopes also illustrates the effects of algae in the basin [56].

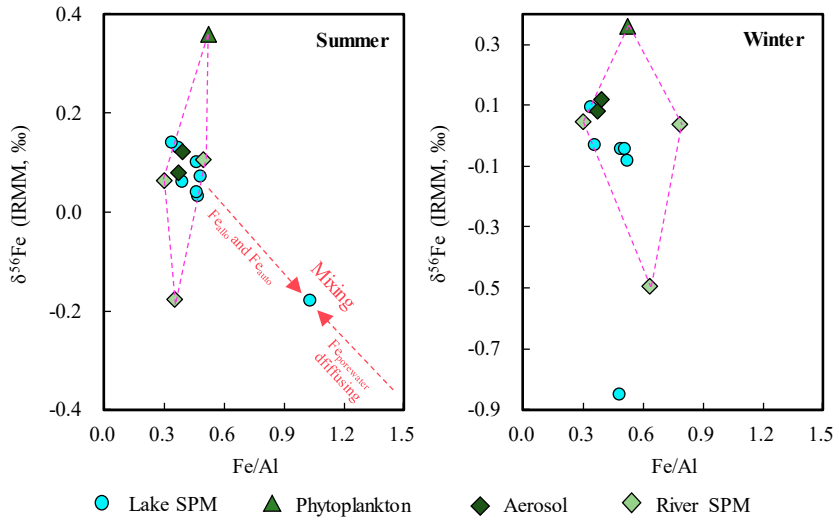

Figure 5. Source analysis of the iron isotope composition of SPM in Hongfeng Lake.

In addition, studies have shown that the iron isotope composition in atmospheric particle is close to the average value of the continental crust, that the $\delta^{56}Fe$ value is between −0.03‰ and 0.24‰, and that the average value is approximately 0.1‰ [49]. The iron isotope composition of SPM in Hongfeng Lake is also affected by atmospheric deposition activities. It is determined that the $\delta^{56}Fe$ value in the atmospheric particles of Hongfeng Lake is 0.08~0.12‰, which is close to the average value of the continental crust, indicating that the area is less affected by human activities, similarly to the results of previous studies [52,57,58]. To further analyse the source, we mapped the possible source ratio of $\delta^{56}Fe$ and Fe/Al and the lake SPM and found that the iron isotopic composition of SPM in lake is affected by the interaction of river input and algae bloom (Figure 5). However, the lowest value of $\delta^{56}Fe$ in the bottom layer of the summer lake is −0.18‰, which indicates that the bottom water is

affected by effects other than the abovementioned autochthonous (algae bloom) and allochthonous (river input) effects. Combined with the conclusion that the dissolved Fe and Mn contents in the bottom lake water were increased significantly, that the δ^{56}Fe value of pore water in the 2 cm sediment of Hongfeng Lake is approximately −0.57‰ indicates that the diffusion of iron in pore water has a certain influence on the water in the bottom of the lake (Figure 5).

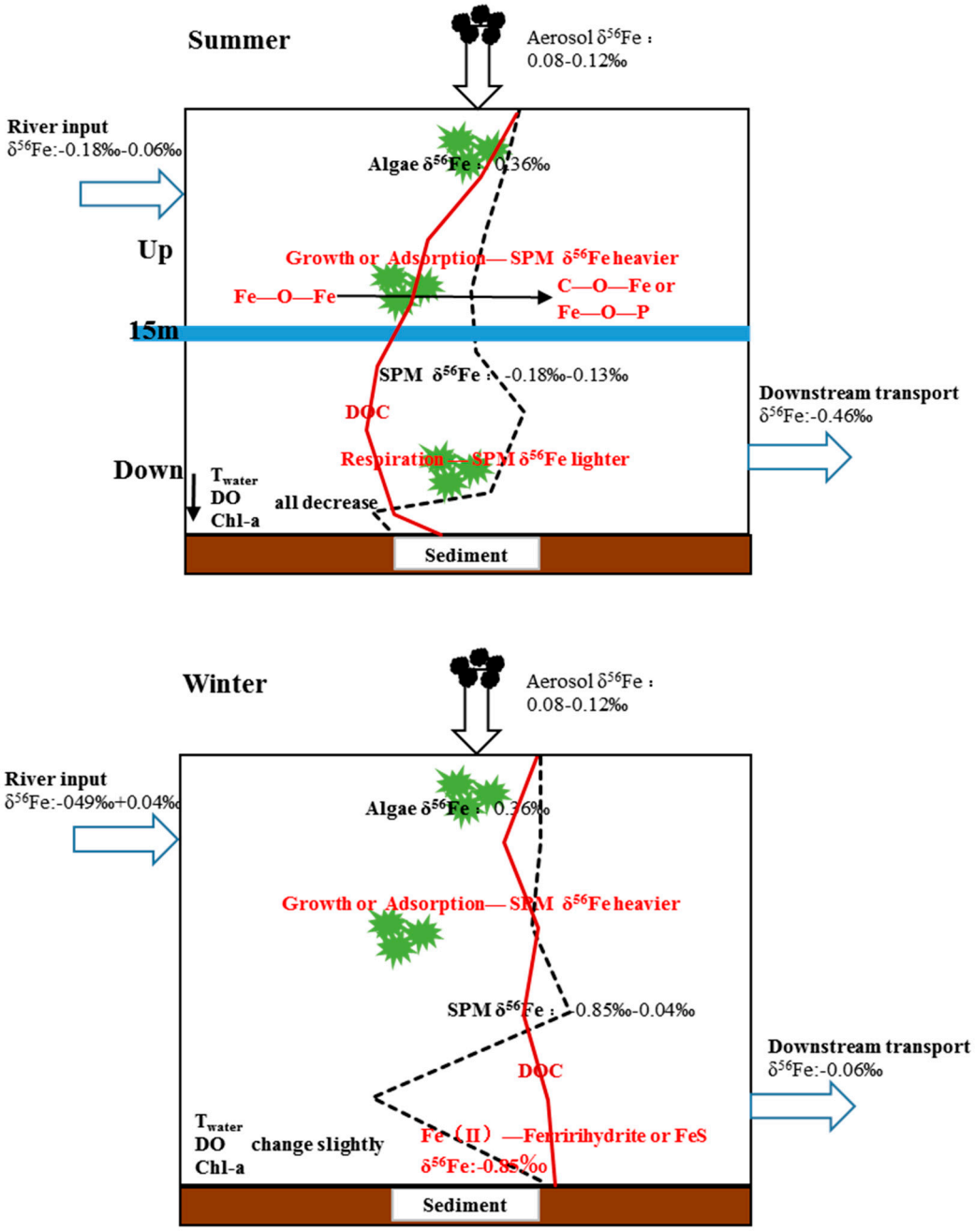

Figure 6. Changes in the iron isotope composition of SPM in the summer and winter in Hongfeng Lake.

4.3. Algae Bloom and Depth-Related Variations on the Iron Isotope Composition of SPM in Hongfeng Lake

The value of δ^{56}Fe in Hongfeng Lake and its inflow tributaries is larger in summer than in winter, and the variation in the δ^{56}Fe value of SPM in the lake with depth is distinct in summer. No obvious change was observed except for a minimum value at a depth of 20 m in winter (Figure 3). As shown in Figures 5 and 6, compared with atmospheric deposition and river input, algae play an important role in controlling the iron isotope composition of SPM, especially in the surface environment, as determined

by comparing the $\delta^{56}Fe$ values of Hongfeng Lake, which vary with depth in winter and summer. In addition, in aquatic ecosystems, algal DOM increases the content of autochthonous natural organic matter (DOM) through extracellular metabolism or intracellular autolysis. The former mainly occurs during the exponential growth period, and the latter mainly occurs during the stable period of algae. In this study, Hongfeng Lake was divided into upper and lower parts at a depth of 15 m. The average DOC content of SPM in the upper water was calculated to be 4.37 $mg \cdot L^{-1}$, and that in the lower part was 4.07 $mg \cdot L^{-1}$. This discrepancy shows that DOC varies to a certain degree between the upper and lower water bodies. The correlation calculation between DOC content and $\delta^{56}Fe$ value in the upper and lower water showed that both R^2 values were 0.98, indicating a high correlation (Figure 4). Additionally, there was a positive correlation at the top and a negative correlation at the bottom, which indicates that the difference in algae metabolism between the upper and lower parts of Hongfeng Lake plays an important role in determining the iron isotopic composition of SPM.

Combined with the trend of chlorophyll-a, it can be observed that the surface of the lake in summer is rich in light and nutrients; thus, the growth and absorption of algae are prominent [52]. During the adsorption of iron on the surface of algae cells, Fe will form stronger covalent heavy metal coordination bonds (Fe–O–C or Fe–O–P) due to the combination of phosphate and carboxyl functional groups on the surface of algae, which is different from the form of the O–Fe–O covalent bond that occurs in aqueous solution (Figure 6). Meanwhile, heavier isotopes are generally more prone to enrichment in species with a higher binding energy. Therefore, with increasing biomass, organic adsorbed iron increases, and the iron isotope composition becomes heavier [59]. In addition, Hongfeng Lake is a moderate trophic seasonal layered lake that hosts blue-green algae; therefore, this study verifies the experimental conclusion of Mulholland et al. [60], which is that blue-green algae produce iron isotope fractionation during iron adsorption and enrich heavy iron isotopes occur on the surface of blue-green algae. According to the study by Sun and Wang [61], in solutions with an Fe content of less than 100 μM, the fractionation result obtained for the iron isotope in the intracellular absorption of algae is expressed as $\Delta^{56}Fe_{intra} < 1.4‰$, and for the extracellular adsorption process, $\Delta^{56}Fe_{extra}$ can be as low as $-2.5‰$. Therefore, due to the influence of extracellular adsorption and intracellular absorption processes, algae will enrich Fe (III) oxides of heavy iron isotopes during the growth of algae [62,63]. Sun and Wang's [61] experiments showed that carbonate formation and deposition of light iron isotopes are enriched during algae growth. The proliferation of surface algae will cause the oxygen content of the lake to decrease with depth, and the concentration of Fe (II) will increase with depth.

In addition, the content of DO is only 1.09 $mg \cdot L^{-1}$, and the Fe/Al ratio reaches 1.04 in the stratified bottom water. Compared with the content observed in the upper water, this value is significantly higher, which indicates that a "ferrous-wheel" cycle forms at the bottom of Hongfeng Lake, which is close to Aha Lake. The difference is that the iron cycle is very active in Aha Lake due to the great influence of river input, which mainly occurs at the sediment-water interface in Hongfeng Lake. To further understand the influence of allochthonous input and autochthonous input on the water iron cycle, the proportion of autochthonous active Fe (III) in the Fe cycle can be roughly calculated by the following formula [19].

$$\delta^{56}Fe_{SPM} = \delta^{56}Fe_{allo} \cdot (1 - f) + \delta^{56}Fe_{auto} \cdot f \quad (3)$$

$$\delta^{56}Fe_{auto} = \Delta^{56}Fe + \delta^{56}Fe_{SRM} \quad (4)$$

$$\delta^{56}Fe_{SRM} = \delta^{56}Fe_{YCR} \cdot J_{YCR} + \delta^{56}Fe_{MXR} \cdot J_{MXR} + \delta^{56}Fe_{HLR} \cdot J_{HLR} \quad (5)$$

where δ^{56}Feallo is the $\delta^{56}Fe$ value of allochthonous inputs; δ^{56}Feauto is the $\delta^{56}Fe$ value of autochthonous reactive Fe (III); $\delta^{56}Fe_{SRM}$ is the $\delta^{56}Fe$ value of the starting reactive Fe oxides δ^{56}Fei and Ji for the Fe isotope composition and ratio of particulate Fe flux of river i to the total particulate Fe flux of the rivers YCR, MXR and HLR; and f is the percentage in the sampled particulates. We take roughly average $\delta^{56}Fe$ values of epilimnetic particulates as those (δ^{56}Feallo = 0.08‰) of allochthonous inputs, including atmospheric and riverine inputs. A fractionation factor of $-1.3‰$ ($\Delta^{56}Fe_{Fe(II)aq–Fe(III)oxide}$)

was used [49,57] to calculate the δ^{56}Fe value of autochthonous reactive Fe (III). It was calculated that in summer, 23% of reactive Fe (III) at a depth of 20 m is produced by the action of autochthonous Fe oxide, which is lower than that in Aha Lake (45%–76%) [25]. According to previous theoretical and experimental studies, Fe (III) tends to enrich heavy iron isotopes more readily than Fe (II) does. According to a study on Fe isotopes in the oxidation process of Fe (II) by Bullen et al. [64], Fe (II) will be preferentially oxidized when Fe $(II)_{aq}$ has a higher δ^{56}Fe value. Additionally, hydrated iron oxides have high iron isotope values, with $\Delta^{56}Fe_{Ferrihydrite\text{-}Fe(II)aq}$ being 0.13‰~1.00‰. Moreover, the formation of iron sulfide minerals will also lead to the fractionation of isotopes, and the value of $\Delta^{56}Fe_{Fe(II)\text{-}FeS}$ is between 0.3‰ and 0.85‰. According to the value (0.3‰) and rough calculation, the proportion of iron sulfide formation in the iron cycle is approximately 3%, indicating that the possibility of S (II) is small in the iron cycle at the bottom of Hongfeng Lake. Therefore, it can be observed that there are lower DO and pH values and a higher content of DOC in the bottom of the water in summer. These conditions may cause most of the Fe oxide to exist in a form that is complexed with organic matter or converted to Fe (II).

5. Conclusions

(1) The ranges of δ^{56}Fe in SPM in Hongfeng Lake and its main tributaries are between −0.85‰ and +0.14‰ and between −0.46‰ and +0.14‰, respectively. Additionally, δ^{56}Fe has a high linear correlation with Fe/Al; thus, the terrestrial material carried by the main tributaries of the lake will have an important effect on the iron sources in the lake. Furthermore, Hongfeng Lake is a moderately eutrophic lake. Algal bloom and the content of chlorophyll a (Chl-a) are high, which, combined with the high correlation between Chl-a and the value of δ^{56}Fe, indicates that the growth of algae has an important influence on the change of iron isotope composition of suspended particulate matter (SPM) in lake water and that the adsorption and growth absorption of Fe by algae is the main reason for the change in the value of δ^{56}Fe; thus, Fe isotope can be used to trace the lake's biological action.

(2) For the lake and its inflow tributaries, δ^{56}Fe values are higher in summer than in winter. The variation in the δ^{56}Fe values of SPM in the lake with depth is more distinct in summer than in winter. According to a linear correlation analysis, the content of dissolved organic carbon (DOC) in Hongfeng Lake's upper and lower water bodies, respectively, is highly correlated with the value of δ^{56}Fe. Specifically, the correlation is positive in the upper water but negative in the bottom water, which indicates that the difference in algae metabolism patterns between the upper and lower water bodies of Hongfeng Lake plays an important role in the iron isotope composition of SPM. The composition of the Fe isotope in SPM is altered by organic adsorption and growth absorption of algae in the upper water. With an increase in depth, the degradation process becomes the main process. In addition, the value of δ^{56}Fe is low and the Fe/Al ratio is high in the bottom water, which indicates that a "ferrous-wheel" cycle forms at the bottom of the water.

Author Contributions: Project administration, Y.T.; Writing–original draft, X.Z.; Writing–review & editing, L.S.

Funding: This research was financially supported by the Natural Science Foundation of China (No. 41473086, No. 41877355).

Conflicts of Interest: The authors declare no conflict of interest.

References

1. Taylor, S.R. Abundance of chemical elements in the continental crust: A new table. *Geochim. Cosmochim. Acta* **1964**, *28*, 1273–1285. [CrossRef]
2. Boyd, P.W.; Ellwood, M.J. The biogeochemical cycle of iron in the ocean. *Nat. Geosci.* **2010**, *3*, 675–682. [CrossRef]
3. Hopkinson, B.M.; Morel, F.M. The role of siderophores in iron acquisition by photosynthetic marine microorganisms. *Biometals* **2009**, *22*, 659–669. [CrossRef] [PubMed]

4. Nagai, T.; Imai, A.; Matsushige, K.; Fukushima, T. Effect of iron complexation with dissolved organic matter on the growth of cyanobacteria in a eutrophic lake. *Aquat. Microb. Ecol.* **2006**, *44*, 231–239. [CrossRef]
5. Bruland, K.W.; Donat, J.; Hutchins, A. Interactive influences of bioactive trace metals on biological production in oceanic waters. *Limno. Oceangr.* **1991**, *36*, 1555–1577. [CrossRef]
6. Chang, C.C.Y.; Kuwabara, J.S.; Pasilis, S.P. Phosphate and iron limitation of phytoplankton biomass in Lake Tahoe. *Can. J. Fish. Aquat. Sci.* **1992**, *49*, 1206–1215. [CrossRef]
7. Davison, W. Iron and manganese in lakes. *Earth Sci. Rev.* **1993**, *34*, 119–163. [CrossRef]
8. Hamilton, T.J.; Davison, W.; Morfett, K. The biogeochemical cycling of Zn, Cu, Fe, Mn, and dissolved organic C in a seasonally anoxic lake. *Limnol. Oceangr.* **1996**, *41*, 408–418. [CrossRef]
9. Staubwasser, M.; Von Blanckenburg, F.; Schoenberg, R. Iron isotopes in the early marine diagenetic iron cycle. *Geology* **2006**, *34*, 629–632. [CrossRef]
10. Fehr, M.A.; Andersson, P.S.; Hålenius, U.; Mörth, C.M. Iron isotope variations in Holocene sediments of the Gotland Deep, Baltic Sea. *Geochim. Cosmochim. Acta* **2008**, *72*, 807–826. [CrossRef]
11. Poitrasson, F.; Viers, J.; Martin, F.; Braun, J.J. Limited iron isotope variations in recent lateritic soils from Nsimi, Cameroon: Implications for the global Fe geochemical cycle. *Chem. Geol.* **2008**, *253*, 54–63. [CrossRef]
12. Zhao, X.; Zhang, H.; Zhu, X.; Tang, S.; Tang, Y. Iron isotope variations in spinel peridotite xenoliths from North China Craton:implications for mantle metasomatism. *Contrib. Mineral. Petrol.* **2009**, *160*, 1–14. [CrossRef]
13. Severmann, S.; Mcmanus, J.; Berelson, W.M.; Hammond, D.E. The continental shelf benthic iron flux and its isotope composition. *Geochim. Cosmochim. Acta* **2010**, *74*, 3984–4004. [CrossRef]
14. Severmann, S.; Lyons, T.W.; Anbar, A.; McManus, J.; Gordon, G. Modern iron isotope perspective on the benthic iron shuttle and the redox evolution of ancient oceans. *Geology* **2015**, *36*, 487–490. [CrossRef]
15. Dauphas, N.; John, S.G.; Rouxel, O. Iron Isotope Systematics. *Rev. Minal. Geochem.* **2017**, *82*, 415–510. [CrossRef]
16. Teutsch, N.; Schmid, M.; Müller, B.; Halliday, A.N.; Bürgmann, H.; Wehrli, B. Large iron isotope fractionation at the oxic–anoxic boundary in Lake Nyos. *Earth Planet. Sci. Lett.* **2009**, *285*, 52–60. [CrossRef]
17. Poitrasson, F.; Vieira, L.C.; Seyler, P.; dos Santos Pinheiro, G.M.; Mulholland, D.S.; Bonnet, M.P.; Martinez, J.-M.; Lima, B.A.; Boaventura, R.; Chmeleff, J.; et al. Iron isotope composition of the bulk waters and sediments from the Amazon River Basin. *Chem. Geol.* **2014**, *377*, 1–11. [CrossRef]
18. Fantle, M.S.; Depaolo, D.J. Iron isotopic fractionation during continental weathering. *Earth Planet. Sci. Lett.* **2004**, *228*, 547–562. [CrossRef]
19. Bergquist, B.A.; Boyle, E.A. Dissolved iron in the tropical and subtropical Atlantic ocean. *Glob. Biogeochem. Cycles* **2006**, *20*, 1–14. [CrossRef]
20. Ingri, J.; Malinovsky, D.; Rodushkin, I.; Baxter, D.C.; Widerlund, A.; Andersson, P.; Gustafsson, Ö.; Forsling, W.; Öhlander, B. Iron isotope fractionation in river colloidal matter. *Earth Planet. Sci. Lett.* **2006**, *245*, 792–798. [CrossRef]
21. Escoube, R.; Rouxel, O.J.; Sholkovitz, E.; Donard, O.F.L. Iron isotope systematics in estuaries: The case of North River, Massachusetts (USA). *Geochim. Cosmochim. Acta* **2009**, *73*, 4045–4059. [CrossRef]
22. Ilina, S.M.; Poitrasson, F.; Lapitskiy, S.A.; Alekhin, Y.V.; Viers, J.; Pokrovsky, O.S. Extreme iron isotope fractionation between colloids and particles of;boreal and temperate organic-rich waters. *Geochim. Cosmochim. Acta* **2013**, *101*, 96–111. [CrossRef]
23. Zhang, R.; John, S.G.; Zhang, J.; Ren, J.; Wu, Y.; Zhu, Z.; Liu, S.; Zhu, X.; Marsay, C.M.; Wenger, F. Transport and reaction of iron and iron stable isotopes in glacial meltwaters on Svalbard near Kongsfjorden: From rivers to estuary to ocean. *Earth Planet. Sci. Lett.* **2015**, *424*, 201–211. [CrossRef]
24. Chen, J.B.; Busigny, V.; Gaillardet, J.; Louvat, P.; Wang, Y.N. Iron isotopes in the Seine River (France): Natural versus anthropogenic sources. *Geochim. Cosmochim. Acta* **2014**, *128*, 128–143. [CrossRef]
25. Song, L.; Liu, C.Q.; Wang, Z.L.; Zhu, X.; Teng, Y.; Liang, L.; Tang, S.; Li, J. Iron isotope fractionation during biogeochemical cycle: Information from suspended particulate matter (SPM) in Aha Lake and its tributaries, Guizhou, China. *Chem. Geol.* **2011**, *280*, 170–179. [CrossRef]
26. Teutsch, N.; Gunten, U.V.; Porcelli, D.; Cirpka, O.A.; Halliday, A.N. Adsorption as a cause for iron isotope fractionation in reduced groundwater. *Geochim. Cosmochim. Acta* **2005**, *69*, 4175–4185. [CrossRef]

27. Dos Santos Pinheiro, G.M.; Poitrasson, F.; Sondag, F.; Vieira, L.C.; Pimentel, M.M. Iron isotope composition of the suspended matter along depth and lateral profiles in the Amazon River and its tributaries. *J. N. Am. Earth Sci.* **2013**, *44*, 35–44. [CrossRef]
28. Klar, J.K.; Schlosser, C.; Milton, J.A.; Woodward, E.M.S.; Lacan, F.; Parkinson, I.J.; Achterberg, E.P.; James, R.H. Sources of dissolved iron to oxygen minimum zone waters on the Senegalese continental margin in the tropical North Atlantic Ocean: Insights from iron isotopes. *Geochim. Cosmochim. Acta* **2018**, *236*, 60–78. [CrossRef]
29. Wang, J.F.; Chen, J.A.; Ding, S.M.; Guo, J.; Christopher, D.; Dai, Z.; Yang, H. Effects of seasonal hypoxia on the release of phosphorus from sediments in deep-water ecosystem: A case study in Hongfeng Reservoir, Southwest China. *Environ. Pollut.* **2016**, *219*, 858–865. [CrossRef] [PubMed]
30. Wang, L.Y.; Zhang, R.Y.; Chen, J.A. Physicochemical characteristics of the overlying water and spatial-temporal distribution of carbon, nitrogen and silicon in Lake Hongfeng, Guizhou Province, China (in Chinese). *Earth Einviron.* **2017**, *45*, 383–389.
31. Nigro, A.; Sappa, G.; Barbieri, M. Application of boron and tritium isotopes for tracing landfill contamination in groundwater. *J. Geochem. Explor.* **2017**, *172*, 101–108. [CrossRef]
32. Boschetti, T.; Awaleh, M.; Barbieri, M. Waters from the Djiboutian Afar: A Review of Strontium Isotopic Composition and a Comparison with Ethiopian Waters and Red Sea Brines. *Water* **2018**, *10*, 1700. [CrossRef]
33. Maréchal, C.N.; Télouk, P.; Albarède, F. Precise analysis of copper and zinc isotopic compositions by plasma-source mass spectrometry. *Chem. Geol.* **1999**, *156*, 51–273. [CrossRef]
34. Suohan, T.; Xiangkun, Z.; Jin, L.; Bin, Y.A.N. Preparation of reference material for Cu, Fe and Zn isotope measurement of geological samples. *Acta Petrol. Mineral.* **2008**, *4*, 279–284.
35. Li, J.; Tang, S.; Zhu, X.; Li, Z.; Li, S.Z.; Yan, B.; Wang, Y.; Sun, J.; Shi, Y.; Dong, A. Basaltic and Solution Reference Materials for Iron, Copper and Zinc Isotope Measurements. *Geostand. Geoanal. Res.* **2018**, *43*, 163–175. [CrossRef]
36. Aizaki, M.; Otsuki, A.; Fukushima, T.; Hosomi, M.; Muraoka, K. Application of Carlson's trophic state index to Japanese lakes and relationships between the index and other parameters. *Proc. Int. Assoc. Theor. Appl. Limnol.* **1981**, *16*, 19–22. [CrossRef]
37. Duan, H.; Zhang, Y.; Zhang, B.; Wang, Z. Assessment of Chlorophyll-a Concentration and Trophic State for Lake Chagan Using Landsat TM and Field Spectral Data. *Environ. Monit. Assess.* **2007**, *129*, 295–308. [CrossRef] [PubMed]
38. Jones, R.I. Vertical distribution and diel migration of flagellated phytoplankton in a small humic lake. *Hydrobiologia* **1988**, *161*, 75–87. [CrossRef]
39. Langenberg, V.T.; Mwape, L.M.; Tshibangu, K.; Tumba, J.M.; Koelmans, A.A.; Roijackers, R.; Salonen, K.; Sarvala, J.; Mölsä, H. Comparison of thermal stratification, light attenuation, and chlorophyll- a dynamics between the ends of Lake Tanganyika. *Aquat. Ecosyst. Health Manag.* **2002**, *5*, 255–265. [CrossRef]
40. Ma, X.; Wang, Y.; Feng, S.; Wang, S. Vertical migration patterns of different phytoplankton species during a summer bloom in Dianchi Lake, China. *Environ. Earth Sci.* **2015**, *74*, 3805–3814. [CrossRef]
41. Waples, J.T.; Klump, J.V. Vertical and horizontal particle transport in the coastal waters of a large lake: An assessment by sediment trap and thorium–234 measurements. *J. Geophys. Res. Oceans* **2013**, *118*, 5376–5397. [CrossRef]
42. Tranvik, L.J. Allochthonous Dissolved Organic-Matter as an Energy-Source for Pelagic Bacteria and the Concept of the Microbial Loop. *Hydrobiologia* **1992**, *229*, 107–114. [CrossRef]
43. Sachse, A.; Henrion, R.; Gelbrecht, J.; Steinberg, C.E.W. Classification of dissolved organic carbon (DOC) in river systems: Influence of catchment characteristics and autochthonous processes. *Org. Geochem.* **2005**, *36*, 923–935. [CrossRef]
44. Hiriart-Baer, V.P.; Fortin, C.; Lee, D.Y.; Campbell, P.G. Toxicity of silver to two freshwater algae, Chlamydomonas reinhardtii and Pseudokirchneriella subcapitata, grown under continuous culture conditions: Influence of thiosulphat. *Aquat. Toxicol.* **2006**, *78*, 136–148. [CrossRef] [PubMed]
45. Malinskyrushansky, N.Z.; Legrand, C. Excretion of dissolved organic carbon by phytoplankton of different sizes and subsequent bacterial uptake. *Mar. Ecol. Progress* **1996**, *132*, 249–255. [CrossRef]
46. Rochelle-Newall, E.J.; Fisher, T.R. Chromophoric dissolved organic matter and dissolved organic carbon in Chesapeake Bay. *Mar. Chem.* **2002**, *77*, 23–41. [CrossRef]

47. Kusakabe, M.; Tiodjio, R.E.; Christenson, B.; Saiki, K.; Ohba, T.; Yaguchi, M. Enrichment of ferrous iron in the bottom water of Lake Nyos. *J. Afr. Earth Sci.* **2018**, *150*, 37–46. [CrossRef]
48. Simmonds, B.; Wood, S.A.; Özkundakci, D.; Hamilton, D.P. Phytoplankton succession and the formation of a deep chlorophyll maximum in a hypertrophic volcanic lake. *Hydrobiologia* **2015**, *745*, 297–312. [CrossRef]
49. Beard, B.L.; Johnson, C.M.; Skulan, J.L.; Nealson, K.H.; Cox, L.; Sun, H. Application of Fe isotopes to tracing the geochemical and biological cycling of Fe. *Chem. Geol.* **2003**, *195*, 87–117.
50. Timmermans, K.R.; Gerringa, L.J.A.; de Baar, H.J.W.; van der Wagt, B.; Veldhuis, M.J.W.; de Jong, J.T.M.; Croot, P.L.; Boye, M. Growth rates of large and small Southern Ocean diatoms in relation to availability of iron in natural seawater. *Limnol. Oceanogr.* **2001**, *46*, 260–266. [CrossRef]
51. Ussher, S.J.; Achterberg, E.P.; Worsfold, P.J. Marine Biogeochemistry of Iron. *Environ. Chem.* **2004**, *1*, 67–80. [CrossRef]
52. Radic, A.; Lacan, F.; Murray, J.W. Iron isotopes in the seawater of the equatorial Pacific Ocean: New constraints for the oceanic iron cycle. *Earth Planet. Sci. Lett.* **2011**, *306*, 1–10. [CrossRef]
53. Zhang, W. *EnvironmentaI Characteristics and Eutrophication of Hongfeng Lake and Baihua Lake*; Guizhou Science and TechnoIogy Press: Guiyang, China, 1999; pp. 20–58. (In Chinese)
54. Xiao, H.Y.; Liu, C.Q.; Li, S.L.; Wang, S.L. Nitrogen biogeochemical cycles in lakes with strong hydraulic power during summer stratification: A case study of Hongfeng Lake in Guizhou Province, Southwest China. *Geochimica* **2002**, *31*, 571–576. (In Chinese)
55. Shaked, Y.; Erel, Y.; Sukenik, A. Phytoplankton-Mediated Redox Cycle of Iron in the Epilimnion of Lake Kinneret. *Environ. Sci. Technol.* **2002**, *36*, 460–467. [CrossRef] [PubMed]
56. Lili, L.; Congqiang, L.; Zhongliang, W. The application of copper and zinc isotope method in environment geochemistry. *Earth Environ.* **2006**, *34*, 81–89.
57. Beard, B.L.; Johnson, C.M.; Von Damm, K.L.; Poulson, R.L. Iron isotope constraints on Fe cycling and mass balance in oxygenated Earth oceans. *Geology* **2003**, *31*, 629–632. [CrossRef]
58. Waeles, M.; Baker, A.R.; Jickells, T.; Hoogewerff, J. Global dust teleconnections: Aerosol iron solubility and stable isotope composition. *Environ. Chem.* **2007**, *4*, 233–237. [CrossRef]
59. González, A.G.; Pokrovsky, O.S.; Jiménez-Villacorta, F.; Shirokova, L.S.; Santana-Casiano, J.M.; González-Dávila, M.; Emnova, E.E. Iron adsorption onto soil and aquatic bacteria: XAS structural study. *Chem. Geol.* **2014**, *372*, 32–45. [CrossRef]
60. Mulholland, D.S.; Poitrasson, F.; Shirokova, L.S.; González, A.G.; Pokrovsky, O.S.; Boaventura, G.R.; Vieira, L.C. Iron isotope fractionation during Fe (II) and Fe (III) adsorption on cyanobacteria. *Chem. Geol.* **2015**, *400*, 24–33. [CrossRef]
61. Sun, R.; Wang, B. Iron isotope fractionation during uptake of ferrous ion by phytoplankton. *Chem. Geol.* **2018**, *481*, 65–73. [CrossRef]
62. Wiesli, R.A.; Beard, B.L.; Johnson, C.M. Experimental detemination of Fe isotope factionation between aquous Fe (II), siderite and "green rust" in abiotic system. *Chem. Geol.* **2005**, *211*, 343–362. [CrossRef]
63. Johnson, C.M.; Roden, E.E.; Welch, S.A.; Beard, B.L. Experimental constraints on Fe isotope fractionation during magnetite and Fe carbonate formation coupled to dissimilatory hydrous ferric oxide reduction. *Geochim. Cosmochim. Acta* **2005**, *69*, 963–993. [CrossRef]
64. Bullen, T.D.; White, A.F.; Childs, C.W.; Vivit, D.V.; Schulz, M.S. Demonstration of significant abiotic iron isotope fractionation in nature. *Geology* **2001**, *29*, 699–702. [CrossRef]